J. Wind Eng. Ind. Aerodyn. 147 (2015) 85–94

Contents lists available at ScienceDirect

Journal of Wind Engineering and Industrial Aerodynamics

journal homepage: www.elsevier.com/locate/jweia

Calculation of rain load based on single raindrop impinging experiment and applications

Xing Fu [a,*], Hong-Nan Li [a], Y.B. Yang [b]

[a] State Key Laboratory of Coastal and Offshore Engineering, Dalian University of Technology, Dalian 116023, China
[b] School of Civil Engineering, Chongqing University, Chongqing 400045, China

ARTICLE INFO

Article history:
Received 19 April 2015
Received in revised form
29 September 2015
Accepted 29 September 2015
Available online 22 October 2015

Keywords:
Piezoelectric transducer
Raindrop impinging force
Rain load
Transmission tower
Wind tunnel test
Typhoon

ABSTRACT

In this paper, a method for calculating the rain load based on the single raindrop impinging experiment is presented, and a wind tunnel test is carried out to validate its effectiveness. The raindrop impinging force is measured using a self-made piezoelectric transducer. Based on the experimental results, a fitting formula of the peak force is proposed, which is then used to normalize the time-history of the raindrop impinging force. According to the experimental results and the law of conservation of momentum, a method is proposed for calculating the rain load in each rainfall event. The final formula derived is then used in the numerical simulation of a transmission tower subjected to the wind and rain loads, and it is demonstrated that the maximum percentage of root-mean-square (RMS) acceleration induced by the rain load relative to the wind load can reach to 22.4% for the basic wind speed of 5 m/s and rain intensity of 200 mm/h, which indicates that the effect of rain load on the tower response is not negligible. Meanwhile a wind tunnel test has been conducted to verify the simulation results and good agreement has been achieved in this regard. Finally, response analysis of transmission tower for a specific location of a recorded typhoon is performed and results reveal that the rain load should be given more attention during a typhoon.

1. Introduction

Rainfall is a common natural phenomenon, which can result in several problems in terms of building physics, such as the surface soiling due to runoff, weathering, algae formation, salt damage and frost damage at exterior wall surfaces, and mold growth at inside wall surfaces (Kubilay et al., 2013). During a typhoon or hurricane, the strong wind is usually accompanied with heavy rainfalls, while the forming mechanism of rain load is still not clear. Historically, numerous structures have collapsed during severe gales and thunderstorms. Most of the time, researchers have attributed the collapses to strong winds (Fu et al., 2015). The effect of rainfall on building physics has attracted lots of attentions (Blocken, 2014; Blocken and Carmeliet, 2004), and yet its effect on the dynamic response of structures has been ignored in design. Thus, it is necessary to study the raindrop impinging force and to propose a rain load model for clarifying its mechanism of formation and for application to structural dynamic analysis.

Mehdi-Nejad et al. (2003) developed a one-field volume of fluid tracking code that can model the motion of multiple fluid phases and then it was applied to simulate the impact of water droplets on a steel surface. Predictions from the model were compared with photographs available in the literature, which showed good agreement. Lunkad et al. (2007) discussed the influence of surface wetting characteristics by using static contact angle (SCA) and dynamic contact angle (DCA) models, and found that the SCA model can predict the drop impact and spreading behavior in quantitative agreement with experiments for the hydrophobic surfaces (SCA $>90^\circ$). Fujimoto et al. (2007) investigated the effect of impact angle on the deformation behavior of droplets and the results showed that the shape of droplet on the surface became increasingly asymmetric with a decreasing impact angle. Sahaya Grinspan and Gnanamoorthy (2010) found that the output signals of transducer obtained from the bead impact tests and liquid drop impact tests were more or less same when the mass of bead was about 8.5 times larger than that of the oil droplet and the height in the droplet impact test was higher than that of bead impact tests, which indicate that the acting mechanisms of bead and liquid drop were totally different and the impact evolution of liquid drop is a very complicated phenomenon.

Li et al. (2012) studied the impact process of a water drop colliding with a rotating disc using a high-speed video camera and results indicated that the tangential velocity at the impact point was a major factor for the occurrence of splash. The objectivity of measurement of droplet impinging on a deformable target may

---

[*] Corresponding author. Tel.: +86 159 4261 4786.
E-mail address: fuxing@mail.dlut.edu.cn (X. Fu).

http://dx.doi.org/10.1016/j.jweia.2015.09.017
0167-6105/© 2015 Elsevier Ltd. All rights reserved.

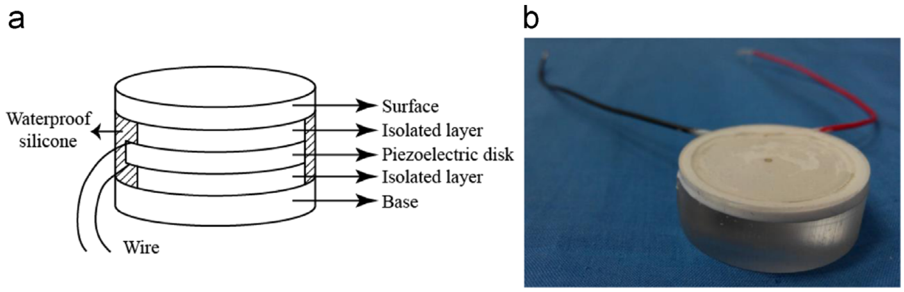

Fig. 1. Piezoelectric transducer: (a) schematic and (b) pictorial view.

sometimes be questioned due to the presence of transducer itself, which is its own dynamic characteristics. By eliminating such measurement errors when necessary, Haboussa et al. (2008) proposed a methodology for exploiting the dynamic test responses to get the true contact pressure sustained by deformable structures during the hydrodynamic impacts.

The stress field of droplet with a high impact speed is very different from low speed results. Haller et al. (2002) observed the fluid dynamics of high-speed (500 m/s) small size (200 μm in diameter) droplet impact on a rigid substrate and results illustrated that the compressibility of the liquid medium plays a dominant role in the evolution of the phenomenon. Li et al. (2011) simulated a simple droplet impingement to a rigid wall using the volume of fluid (VOF) model, adopting three high velocities for the impact: 300 m/s, 400 m/s and 500 m/s. Their results declared that the critical maximum pressure is not highest at the center of droplet contact on the surface at the first instantaneous moment, but the highest at the instant just before the jet eruption and after the contact angle. In the last stages of steam turbines, large droplets (so-called coarse water) were generated from the wet steam flow. These droplets collided with the following rotating blades with almost the peripheral speed of the rotor and this high speed impact was perceived in the form of erosion of low pressure steam turbine blades. Li et al. (2008) and Zhou et al. (2008) derived the governing equations of the transient pressure field in the liquid drop based on a nonlinear wave model and then they calculated the most dangerous impact load/duration time and the most likely crack positions. Ahmad et al. (2009) investigated the droplet impact erosion resistance of five different, but highly relevant, steam turbine blade materials with the help of an erosion test rig. A simplified, but functional, model was then inferred from the test data for estimating the droplet impact erosion resistance of alternative steel and titanium blade materials relative to the materials discussed in this paper. Moreover, they confirmed that the erosion increases with the increase of droplet size and the volume loss per droplet impact increases with the droplet size by a simple power law relation (Ahmad et al., 2013).

Meanwhile, some researchers studied the rain load on tall structures. Li et al. (2013a) proposed an approach for the rain load on the transmission tower, and carried out the dynamic response analyses and experiments of transmission tower under the wind and rain loads. Their results showed that the proposed approach agreed well with the wind tunnel test and the rain load influence on the transmission towers should not be ignored for strong rainstorms. Fu et al. (2014) modified the rain load model proposed by Li et al. (2013a) and the wind tunnel test revealed that the rain load could not be neglected during severe gales and thunderstorms. By simulating the motion of a single raindrop, Fu et al. (2015) validated and explained the phenomenon that the horizontal velocity of raindrop was larger than the corresponding wind speed, and then the velocity difference was introduced to further modify the rain load formula.

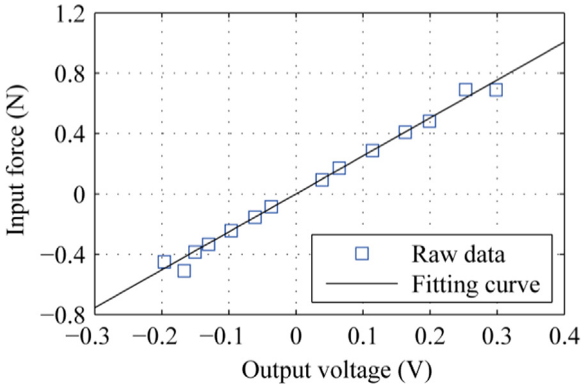

Fig. 2. Calibration curve of the manufactured transducer.

A review of the abovementioned works indicates that most researchers have focused on the deformation evolution and pressure of raindrop impact. Although some models have been proposed for the rain load, most of them work for the simplest conditions. Many factors, such as the motion of impinging raindrop, raindrop splashing and raindrop acceleration, were all ignored. As such, large errors may be encountered when using these models. To fill out such a gap, it is necessary to establish a rain load model by experimental means, considering the effect of various parameters. In Section 2, the single raindrop impinging force will be measured using a self-made transducer. Then the experimental results will be normalized in Section 3, followed by the proposal of a rain load model in Section 4. Such a model will be applied in the numerical analysis of a transmission tower subjected to wind and rain loads in Section 5. A validation of the rain load model by the wind tunnel test is presented in Section 6. In Section 7 the response of the transmission tower induced by a recorded typhoon using the proposed rain load model will be analyzed. Section 8 concludes the study.

2. Experimental study on single raindrop impinging force

2.1. Load transducer

The piezoelectric transducer used is made of a piezoelectric ceramic disk, as shown in Fig. 1. Note that Fig. 1a is only a schematic and does not denote the real scale. The diameter and thickness of the disk are 30 and 0.3 mm, respectively. The diameter of the transducer surface is 35 mm. The waterproof silicone is used to ensure that the transducer can work when it is wetted during the experiment. Calibration tests were conducted with the resulting curve shown in Fig. 2.